New Journal of Physics
The open access journal at the forefront of physics
Deutsche Physikalische Gesellschaft DPG | IOP Institute of Physics

Quantum fluctuations in modulated nonlinear oscillators

Vittorio Peano[1] **and M I Dykman**[2]

[1] Institute for Theoretical Physics II, University of Erlangen-Nuremberg, D-91058 Erlangen, Germany
[2] Department of Physics and Astronomy, Michigan State University, East Lansing, MI 48824, USA
E-mail: vittorio.peano@physik.uni-erlangen.de and dykman@pa.msu.edu

Received 8 July 2013, revised 22 September 2013
Accepted for publication 8 October 2013
Published 10 January 2014

New Journal of Physics **16** (2014) 015011

doi:10.1088/1367-2630/16/1/015011

Abstract

We use a modulated oscillator to study quantum fluctuations far from thermal equilibrium. A simple but important nonequilibrium effect that we discuss first is quantum heating, where quantum fluctuations lead to a finite-width distribution of a resonantly modulated oscillator over its quasienergy (Floquet) states. We also discuss the recent observation of quantum heating. We analyze large rare fluctuations responsible for the tail of the quasienergy distribution and switching between metastable states of forced vibrations. We find the most probable paths followed by the quasienergy in rare events, and in particular in switching. Along with the switching rates, such paths are observable characteristics of quantum fluctuations. As we show, they can change discontinuously once the detailed balance condition is broken. A different kind of quantum heating occurs where oscillators are modulated nonresonantly. Nonresonant modulation can also cause oscillator cooling. We discuss different microscopic mechanisms of these effects.

1. Introduction

The last few years have seen an upsurge in interest in the dynamics of modulated nonlinear oscillators [1]. There have emerged several new areas of research where this dynamics plays a central role, such as nanomechanics, cavity optomechanics and circuit quantum

electrodynamics. Vibrational systems of the new generation are mesoscopic. On the one hand, they can be individually accessed, similar to macroscopic systems, and are well-characterized. On the other hand, since they are small, they experience comparatively strong fluctuations of thermal and quantum origin. This makes their dynamics interesting on its own and also enables using modulated oscillators to address a number of fundamental problems of physics far from thermal equilibrium.

Many nontrivial aspects of oscillator dynamics are related to the nonlinearity. Essentially all currently studied mesoscopic vibrational systems display nonlinearity. For weak damping, even small nonlinearity becomes important. It makes the frequencies of transitions between adjacent oscillator energy levels different. Where several levels are occupied, whether thermally or because of the external modulation, the dynamics strongly depends on the interrelation between the width of the ensuing frequency comb and the oscillator decay rate. As a consequence, a weakly damped nonlinear oscillator can have coexisting states of forced vibrations, i.e. display bistability, already for small amplitudes of resonant modulation [2].

One of the general physics problems addressed with modulated nonlinear oscillators is fluctuation-induced switching in systems that lack detailed balance, see [3–14] for the classical and [15–26] for the quantum regime. A remarkable property of the switching rate $W_{\rm sw}$ in the quantum regime is fragility. The rate calculated for $T = 0$, where the system has detailed balance [27], is exponentially different from the rate calculated for $T > 0$, where the detailed balance is broken [15, 18]. Recently the effect of fragility of the rates of rare events was also found in the problem of population dynamics [28]. There, too, a small change of the control parameter (infinitesimal, in the semiclassical limit) leads to an exponentially strong rate change. The nature of the dynamics and the sources of fluctuations in a quantum oscillator and in population dynamics are totally different, and it is important to understand how it happens that they display common singular features.

An important source of quantum fluctuations, in particular those causing switching, is the coupling of the oscillator to a thermal bath. The immediate result is oscillator relaxation via emission of excitations in the bath accompanied by transitions between the oscillator energy levels. The transitions lead to relaxation only on average, in fact they happen at random, giving rise to peculiar quantum noise. For a resonantly modulated oscillator, the noise causes diffusion over the oscillator quantum states in the external field, which are the quasienergy (Floquet) states. As a result, even where the bath temperature is $T = 0$, the distribution over the states has a finite width, the effect of quantum heating [29].

We discuss quantum heating for a resonantly modulated oscillator and compare the predictions with the recent experiment [30] where the effect was observed. We describe how quantum heating manifests itself in the oscillator spectral characteristics of interest for sideband spectroscopy, the technique nicely implemented in the experiment [30] using a microwave cavity with an embedded qubit. The analysis is based on a minimalist model of the coupling of the oscillator to the spectrometer.

We also study switching between the stable states of forced vibrations of an oscillator modulated close to its eigenfrequency. As quantum heating, switching occurs because of the quantum-noise induced diffusion over the oscillator states. It recalls thermally activated switching of a classical Brownian particle over the potential barrier due to diffusion over energy [31], except that it is due to quantum noise, and therefore is called quantum activation. Generally, the rate of quantum activation largely exceeds the rate of switching via quantum tunneling. We develop an approach to calculating the rate of quantum activation, which naturally

connects to the conventional formulation of the rare events theory in chemical and biological reaction systems and in population dynamics [32, 33]. This approach provides a new insight into the fragility of the switching rate of the oscillator. It also reveals a hitherto unappreciated observable characteristic, the most probable path followed by quasienergy in a fluctuation leading to switching.

The interplay of periodic modulation and fluctuations in a thermal reservoir leads to different quantum effects if the modulation is nonresonant. Such modulation can open a new channel for oscillator relaxation, where a transition between the oscillator energy levels is accompanied by emission (absorption) of excitations in the medium, while the energy deficit is compensated by the modulation. The outcome can be again heating of the oscillator, but very different from the quantum heating outlined above as well as from the conventional Joule heating. Another outcome, that has attracted much attention recently in cavity optomechanics, is oscillator cooling. Pumping an oscillator into a regime of self-sustained vibrations is also possible. We outline major mechanisms that can lead to these effects in different vibrational systems, show that they can be treated in a unified way, and explain the distinction from the effects of resonant modulation.

2. Quasienergy spectrum and the master equation for resonant modulation

2.1. Hamiltonian in the rotating frame

The major nonlinearity mechanism of interest for the effects we will discuss is the Duffing nonlinearity, where the potential energy has a term quartic in the oscillator displacement q; in quantum optics, it corresponds to the Kerr nonlinearity. The simplest types of resonant modulation that lead to the bistability of the oscillator are additive modulation at frequency $\omega_{\rm F}$ close to the oscillator eigenfrequency ω_0 and parametric modulation (modulation of the oscillator frequency) at frequency $\approx 2\omega_0$ [2]. The analysis of quantum fluctuations for these two modulation types has much in common [34], and the method that we will develop here applies to both of them. For concreteness, we will consider here additive modulation. The oscillator Hamiltonian is

$$H_0 = \tfrac{1}{2}p^2 + \tfrac{1}{2}\omega_0^2 q^2 + \tfrac{1}{4}\gamma q^4 + H_{\rm F}(t), \quad H_{\rm F} = -qA\cos\omega_{\rm F} t, \tag{1}$$

where q and p are the oscillator coordinate and momentum, the mass is set equal to one, γ is the anharmonicity parameter and A is the modulation amplitude. We assume that the modulation is resonant and not too strong, so that

$$|\delta\omega| \ll \omega_0, \quad \delta\omega = \omega_{\rm F} - \omega_0, \quad |\gamma|\langle q^2\rangle \ll \omega_0^2. \tag{2}$$

A periodically modulated oscillator is described by the Floquet, or quasienergy, states $\Psi_\varepsilon(t)$. They provide a solution of the Schrödinger equation $\mathrm{i}\hbar\partial_t\Psi = H_0(t)\Psi$ that satisfies the condition $\Psi_\varepsilon(t+t_{\rm F}) = \exp(-\mathrm{i}\varepsilon t_{\rm F}/\hbar)\Psi_\varepsilon(t)$, where $t_{\rm F} = 2\pi/\omega_{\rm F}$. This expression defines quasienergy ε. To find quasienergies and to describe the oscillator dynamics it is convenient to change to the rotating frame. This is done by the standard canonical transformation $U(t) = \exp(-\mathrm{i}a^\dagger a\,\omega_{\rm F} t)$, where $a^\dagger$ and a are the raising and lowering operators of the oscillator. We introduce slowly varying dimensionless coordinate Q and momentum P in the rotating frame

$$U^\dagger(t)qU(t) = C(Q\cos\varphi + P\sin\varphi), \quad U^\dagger(t)pU(t) = -C\omega_{\rm F}(Q\sin\varphi - P\cos\varphi).$$

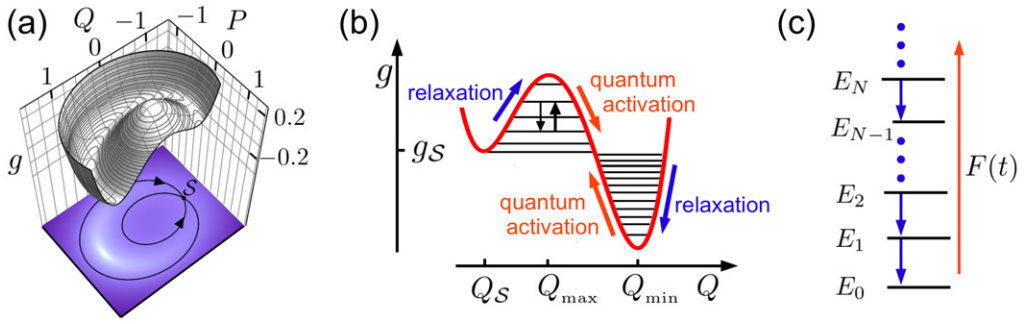

Figure 1. (a) The Hamiltonian function in the rotating frame in the RWA. The extrema of $g(Q, P)$ correspond to the stable vibrational states in the limit of weak damping. (b) The cross-section $g(Q, 0)$ and the quasienergy levels of the states localized about the extrema of $g(Q, P)$. Points $Q_{\min}$, $Q_{\max}$ and Q_S indicate the positions of the minimum, the local maximum and the saddle point of $g(Q, P)$, respectively. The plots refer to $\beta = 0.01$ and $\lambda = 0.041$. (c) The transitions between the Fock states of the oscillator with energies $E_N \approx \hbar\omega_0(N + 1/2)$ accompanied by emission of excitations in the bath, e.g. photons. Some of the corresponding transitions between quasienergy states are shown by small arrows in (b). The stationary state of the oscillator is formed on balance between relaxation and excitation by periodic modulation $F(t)$.

Here, $\varphi = \omega_F t$ and the scaling factor is $C = |8\omega_F(\omega_F - \omega_0)/3\gamma|^{1/2}$. The commutation relation between P and Q has the form

$$[P, Q] = -i\lambda, \quad \lambda = \hbar/(\omega_F C^2) \equiv 3\hbar|\gamma|/8\omega_F^2|\omega_F - \omega_0|. \tag{3}$$

Parameter $\lambda \propto \hbar$ plays the role of the Planck constant in the quantum dynamics in the rotating frame. It is determined by the oscillator nonlinearity, $\lambda \propto \gamma$. For concreteness we assume that $\gamma, \delta\omega > 0$; the oscillator displays bistability for $\gamma\delta\omega > 0$.

In the range (2) the oscillator dynamics can be studied in the rotating wave approximation (RWA). The RWA Hamiltonian is

$$\tilde{H}_0 = U^\dagger H_0 U - i\hbar U^\dagger \dot{U} \approx \tfrac{3}{8} E_{sl}\hat{g},$$
$$g(Q, P) = \tfrac{1}{4}\left(P^2 + Q^2 - 1\right)^2 - \beta^{1/2} Q, \quad \beta = 3|\gamma|A^2/32\omega_F^3|\omega_F - \omega_0|^3, \tag{4}$$

where β is the scaled modulation intensity and $E_{sl} = \gamma C^4$ is the characteristic energy of motion in the rotating frame. This motion is slow on the time scale ω_F^{-1}. Note that E_{sl} is small compared to the vibration energy in the lab frame, $E_{sl} \ll \omega_0^2\langle q^2\rangle \sim \omega_0^2 C^2$.

Operator $\hat{g} = g(Q, P)$ is the dimensionless Hamiltonian in the rotating frame. In the RWA, the Schrödinger equation for the RWA wave function $\psi(Q)$ in dimensionless slow time τ reads

$$i\lambda\dot{\psi} \equiv i\lambda\partial_\tau\psi = \hat{g}\psi, \quad \tau = t|\delta\omega| \equiv \tfrac{3}{8}(\lambda E_{sl}/\hbar)t. \tag{5}$$

Operator $\hat{g}$ is independent of time and has a discrete spectrum, $\hat{g}|n\rangle = g_n|n\rangle$. The eigenvalues g_n give the quasienergies in the RWA, $\varepsilon_n = (3E_{sl}/8)g_n$ (we are using an extended ε-axis rather than limiting ε to the analogue of the first Brillouin zone, which can be defined as $-\hbar\omega_F/2 \leqslant \varepsilon < \hbar\omega_F/2$). Function $g(Q, P)$ has the shape of a tilted Mexican hat and is shown in figure 1(a); the quasienergy levels are shown in figure 1(b).

In contrast to the Hamiltonian H_0, $\hat{g}$ is not a sum of the kinetic and potential energies. As seen from figure 1, the eigenstates localized near the local maximum of $g(Q, P)$ correspond to semiclassical orbits on the surface of the 'inner dome' of $g(Q, P)$; these states become more strongly localized as g_n *increases* toward the local maximum of $g(Q, P)$. The quasienergy level spacing $\propto \lambda E_{\rm sl} \sim \hbar|\delta\omega|$ is small compared to the distance between the oscillator energy levels in the absence of modulation, $|\varepsilon_n - \varepsilon_{n+1}| \sim \lambda E_{\rm sl} \ll \hbar\omega_0$.

2.2. Master equation for linear coupling to the bath

The analysis of the oscillator dynamics is often done assuming that the oscillator is coupled to a thermal bath in such a way that the coupling energy is linear in the oscillator coordinate q and thus in the oscillator ladder operators a, $a^\dagger$ [35]. In this case the coupling energy H_i and the typical relaxation rate Γ are of the form

$$H_i = ah_{\rm b} + a^\dagger h_{\rm b}^\dagger, \quad \Gamma \equiv \Gamma(\omega_0) = \hbar^{-2}\,{\rm Re}\int_0^\infty {\rm d}t\,\langle[h_{\rm b}^\dagger(t), h_{\rm b}(0)]\rangle_{\rm b}\,{\rm e}^{{\rm i}\omega_0 t}, \tag{6}$$

where $h_{\rm b}$ depends on the bath variables only and $\langle\ldots\rangle_{\rm b}$ denotes thermal averaging over the bath states. Relaxation (6) corresponds to transitions between neighboring energy levels of the oscillator in the lab frame, with energy transferred to bath excitations, see figure 1(c). The renormalization of ω_0 due to the coupling is assumed to have been incorporated. For currently studied mesoscopic oscillators of utmost interest is weak coupling, $\Gamma \ll \omega_0$ [1]. It is in this case that even a comparatively weak resonant modulation can lead to strong nonlinear quantum effects.

For a smooth density of states of the bath, resonant modulation does not change the decay rate parameter, $\Gamma(\omega_{\rm F}) \approx \Gamma(\omega_0)$. However, it excites the oscillator, as sketched in figure 1(c). In a stationary state of forced vibrations (in the laboratory frame) the energy provided by the modulation is balanced by the relaxation.

To second order in the interaction (6), the master equation for the oscillator density matrix ρ in dimensionless time $\tau = t|\delta\omega|$ reads

$$\begin{aligned}
&\dot{\rho} \equiv \partial_\tau\rho = {\rm i}\lambda^{-1}[\rho, \hat{g}] - \hat{\kappa}\rho,\\
&\hat{\kappa}\rho = \kappa(\bar{n}+1)(a^\dagger a\rho - 2a\rho a^\dagger + \rho a^\dagger a) + \kappa\bar{n}(aa^\dagger\rho - 2a^\dagger\rho a + \rho aa^\dagger),\\
&\kappa = \Gamma/|\omega_{\rm F} - \omega_0|.
\end{aligned} \tag{7}$$

Here, the term $\propto [\rho, \hat{g}]$ describes dissipation-free motion, cf (5). Operator $\hat{\kappa}\rho$ describes dissipation and has the same form as in the absence of oscillator modulation [36, 37]; κ is the dimensionless decay rate and $\bar{n}$ is the oscillator Planck number,

$$a = (2\lambda)^{-1/2}(Q + {\rm i}P), \quad \bar{n} \equiv \bar{n}(\omega_0) = [\exp(\hbar\omega_0/k_{\rm B}T) - 1]^{-1}. \tag{8}$$

In the classical limit $\lambda \to 0$ the oscillator described by (7) can have one or two stable states of forced vibrations. Their positions in the rotating frame $(Q_{\rm a}, P_{\rm a})$ are given by the stable stationary solutions of the classical equations of motion of the oscillator

$$\dot{Q} = \partial_P g - \kappa Q, \quad \dot{P} = -\partial_Q g - \kappa P. \tag{9}$$

Equation (9) is, essentially, the mean-field equation for the moments ${\rm Tr}(Q\rho)$, ${\rm Tr}(P\rho)$ for $\lambda \to 0$. For small damping $Q_{\rm a}$ and $P_{\rm a}$ are close to the extrema of $g(Q, P)$.

3. Quantum heating

3.1. Balance equation

We will concentrate on the oscillator dynamics in the case where the oscillator is strongly underdamped and its motion is semiclassical,

$$\lambda \ll 1, \quad \kappa \ll 1. \tag{10}$$

In this case the number of quasienergy states localized about the extrema of $g(Q, P)$ is large, $\propto 1/\lambda$ (the scaled quasienergies of such states g_n lie between the value of g at the corresponding extremum and the saddle point value g_S of $g(Q, P)$ in figure 1). In addition, the spacing between the levels is large compared to their width, $|g_n - g_{n\pm1}| \gg \lambda\kappa$. Where the latter condition is met, the off-diagonal matrix elements of the density matrix on the quasienergy states $\rho_{nm} \equiv \langle n|\rho|m\rangle$ $(n \neq m)$ are small, as seen from equation (7). To the lowest order in κ the oscillator dynamics can be described by the balance equation for the populations ρ_{nn} of quasienergy states. From (7)

$$\dot{\rho}_{nn} = \sum_m (W_{mn}\rho_{mm} - W_{nm}\rho_{nn}), \quad W_{mn} = 2\kappa\left[(\bar{n}+1)|a_{nm}|^2 + \bar{n}|a_{mn}|^2\right]. \tag{11}$$

Here, W_{mn} are the rates of interstate transitions; $a_{nm} \equiv \langle n|a|m\rangle$. We disregard tunneling when defining functions $|n\rangle \equiv \psi_n(Q)$, i.e. we use the wave functions localized about the extrema of $g(Q, P)$; the effect of tunneling is exponentially small for $\lambda \ll 1$ and $|n-m| \ll \lambda^{-1}$. We count the localized states off from the corresponding extremum, i.e. for a given extremum the state with $n = 0$ has g_n closest to $g(Q, P)$ at the extremum.

An important feature of the rates W_{mn} is that, even for $T = 0$ (and thus $\bar{n} = 0$), there are transitions both *toward* and *away from* the extrema of $g(Q, P)$. This is because the wave functions $|n\rangle$ are linear combinations of the wave functions of the oscillator Fock states, see figure 1(c). Therefore, even though relaxation corresponds to transitions down in the oscillator energy in figure 1(c), the transitions up and down the quasienergy have nonzero rates. One can show that, for both extrema of $g(Q, P)$, for states localized about an extremum the rates of transitions toward the extremum are larger than away from it. Therefore, depending on where the system was prepared initially, it would most likely move to one or the other extremum of $g(Q, P)$. This is why the extrema correspond to the stable states of forced vibrations of the modulated oscillator in the classical limit of a large number of localized states.

For small effective Planck constant $\lambda \ll 1$, the rates W_{mn} are determined by the matrix elements a_{mn} calculated in the WKB approximation [15, 38]. Such calculation requires an analysis of classical conservative motion with Hamiltonian $g(Q, P)$ and with equations of motion of the form $\dot{Q} = \partial_P g$, $\dot{P} = -\partial_Q g$. A significant simplification comes from the fact that the classical trajectories $Q(\tau; g)$ are described by the Jacobi elliptic functions. As a result, $Q(\tau; g)$ is double-periodic on the complex-τ plane, with real period $\tau_p^{(1)}(g)$ and complex period $\tau_p^{(2)}(g)$. For $|m-n| \ll \lambda^{-1}$ the matrix element a_{mn} is given by the Fourier $m-n$ component of the function $a(\tau; g_n) = (2\lambda)^{-1/2}[Q(\tau; g_n) + iP(\tau; g_n)]$ [39]. It can be calculated along an appropriately chosen closed contour on the complex τ-plane and is determined by the pole of $a(\tau; g_n)$. In particular, for the states localized about the local maximum of $g(Q, P)$ we obtain

$$|a_{n+k\,n}|^2 = \frac{k^2\nu_n^4}{2\beta\lambda}\frac{\exp[k\nu_n\,\mathrm{Im}\,(2\tau_* - \tau_p^{(2)})]}{|\sinh[ik\nu_n\,\tau_p^{(2)}/2]|^2}, \quad \nu_n \equiv \nu(g_n) = 2\pi/\tau_p^{(1)}(g_n). \tag{12}$$

Here, $\tau_* \equiv \tau_*(g_n)$ and $\tau_p^{(2)} \equiv \tau_p^{(2)}(g_n)$ [Im τ_*, Im $\tau_p^{(2)} > 0$]; $\tau_*(g)$ is the pole of $Q(\tau; g)$ closest to the real axis; $\nu(g)$ is the dimensionless frequency of vibrations in the rotating frame for the value of the effective Hamiltonian $g(Q, P) = g$. To the leading order in λ, we have $W_{n\,n+k} = W_{n-k\,n}$ for $n, n \pm k \gg 1$.

3.2. Effective temperature of vibrations about a stable state

Equation (12) has to be modified for states very close to the extrema of $g(Q, P)$. Near these extrema the classical motion of the oscillator in the rotating frame is harmonic vibrations. One can introduce raising and lowering operators b and $b^\dagger$ for these vibrations (via squeezing transformation) and expand $g(Q, P)$ near an extremum as

$$\begin{aligned} &Q - Q_\mathrm{a} + \mathrm{i}P = (2\lambda)^{1/2}(b\cosh\varphi_* - b^\dagger \sinh\varphi_*), \\ &\hat{g} \approx g(Q_\mathrm{a}, 0) + \lambda\nu_0\left(b^\dagger b + 1/2\right)\mathrm{sgn}\partial_Q^2 g, \quad \nu_0 = \left|\partial_Q^2 g \partial_P^2 g\right|^{1/2}. \end{aligned} \tag{13}$$

($(Q_\mathrm{a}, P = 0)$ is the position of the considered extremum; it is given by equation $\partial_Q g = Q(Q^2 - 1) - \beta^{1/2} = 0$.) The derivatives of g in (13) are evaluated at $(Q_\mathrm{a}, P = 0)$. Parameter ϕ_* is given by equation $\tanh\varphi_* = (|\partial_Q^2 g|^{1/2} - |\partial_P^2 g|^{1/2})/(|\partial_Q^2 g|^{1/2} + |\partial_P^2 g|^{1/2})$.

From (11) and (13), near an extremum of g we have

$$\begin{aligned} &W_{m+1\,m} = 2\kappa(m+1)(\bar{n}_\mathrm{e} + 1), \quad W_{m\,m+1} = 2\kappa(m+1)\bar{n}_\mathrm{e}, \\ &\bar{n}_\mathrm{e} = \bar{n}\cosh^2\phi_* + (\bar{n}+1)\sinh^2\phi_*, \end{aligned} \tag{14}$$

whereas $W_{m\,m+k} = 0$ for $|k| > 1$. Equation (14) is a familiar expression for the transition rates between the states of an auxiliary harmonic oscillator coupled to a thermal bath, with $\bar{n}_\mathrm{e}$ being the Planck number of the excitations of this bath at the frequency of vibrations near the extremum of $g(Q, P)$ in the rotating frame $\nu_0\delta\omega$.

From (14), the stationary distribution of the original modulated oscillator over its quasienergy states near an extremum of $g(Q, P)$ is of the Boltzmann type, $\rho_{mm} \propto \exp(-g_m/\mathcal{T}_\mathrm{e})$, with effective dimensionless temperature $\mathcal{T}_\mathrm{e} = \lambda\nu_0/\ln[(\bar{n}_\mathrm{e}+1)/\bar{n}_\mathrm{e}]$. In agreement with the qualitative picture discussed above, this temperature is nonzero even where the temperature of the true bath is $T = 0$. This is the effect of quantum heating due to quantum fluctuations in a nonequilibrium system [18, 24, 29, 34].

3.3. Discussion of experiment

Quantum heating of a resonantly modulated nonlinear oscillator was recently observed in an elegant experiment [30] in which the oscillator was a mode of the microwave cavity with an embedded Josephson junction [40]. The occupation of excited quasienergy states of the mode was detected by coupling it to a two-level system (qubit). There was an extra field applied $\propto F_\mathrm{q}\cos\omega_\mathrm{q} t$ at frequency ω_q close to the transition frequency of the qubit ω_ge, and then the resulting population of the excited qubit state was measured as a function of ω_q. The frequency range was chosen in such a way that $|\omega_0 - \omega_\mathrm{q}| \gg |\omega_\mathrm{q} - \omega_\mathrm{ge}|$. Therefore transitions between the qubit states accompanied by transitions between the Fock states of the oscillator (the mode), i.e. emission/absorption of a mode photon, had negligible probability.

A simple way to describe the observations is to think that the oscillator modulates the coupling of the qubit to the field F_q. Then phenomenologically one can write the effective Hamiltonian of the driven qubit as

$$H_q = \tfrac{1}{2}\hbar\omega_{ge}\sigma_z - \tfrac{1}{4}\left[F_q \exp(i\omega_q t)\sigma_-(1+\alpha_q\hat{n}) + \text{H.c.}\right], \quad \hat{n} = a^\dagger a, \tag{15}$$

where σ_z, $\sigma_\pm = \sigma_x \pm i\sigma_y$ are Pauli matrices (operators in the qubit space); H.c. stands for Hermitian conjugate.

Model (15) is minimalist, we keep only the terms that are resonant. In the absence of the field $\propto F_q$ operator $\sigma_-\hat{n}$ in the Heisenberg representation oscillates at frequencies close to ω_{ge} and thus to ω_q; this is the operator of the lowest order in Q, P that behaves like this. The only parameter of the model, α_q, is phenomenological and drops out of the final result. The same description of the effect of the modulation applies to dispersive coupling of the qubit and the oscillator, with the coupling energy $\propto \sigma_z\hat{n}$ independent of the modulation. If this coupling is weak, the coupling parameter just renormalizes α_q in the expression for the qubit transition rate given below. A detailed analysis of the microscopic model will be performed by Ong *et al* [30]. In contrast to [30] we do not assume that the sideband spectrum is a superposition of two equal-width Lorentzians.

The coupling $\propto \alpha_q$ leads to field-induced transitions between the qubit states (caused by operator σ_-), which are accompanied by transitions between the oscillator quasienergy levels (caused by operator $\hat{n}$). The picture is similar to that discussed in section 5, cf figure 4 below. We will assume that the decay rate of the oscillator is larger than the decay rate of the qubit. Then, to the second order in α_q, the contribution to the rate of qubit excitation $|\downarrow\rangle \to |\uparrow\rangle$ due to the qubit–oscillator coupling is given by $(2\hbar)^{-1}|\alpha_q F_q|^2\Phi_{\hat{n}\hat{n}}(\omega_q - \omega_{ge})$. Here, $\Phi_{\hat{n}\hat{n}}(\omega)$ is the power spectrum of the occupation number operator $\hat{n}$. The major contribution to this power spectrum comes from small-amplitude fluctuations about the stable states of forced vibrations of the oscillator. Therefore function $\Phi_{\hat{n}\hat{n}}(\omega)$ has peaks at frequencies $\pm\nu_0|\delta\omega|$ (and generally $\pm 2\nu_0|\delta\omega|$, with smaller amplitude). It is calculated in the appendix. It follows from the result, in particular, that for small damping, $\kappa \ll \nu_0$, the ratio of the peaks of $\Phi_{\hat{n}\hat{n}}(\omega)$ at $\omega = \nu_0|\delta\omega|$ and $\omega = -\nu_0|\delta\omega|$ is given by the factor $(\bar{n}_e + 1)/\bar{n}_e$, i.e. it provides a direct measure of the effect of quantum heating.

The coupling $\propto \alpha_q$ also leads to downward field-induced qubit transitions $|\uparrow\rangle \to |\downarrow\rangle$. However, for a comparatively weak field F_q transitions $|\uparrow\rangle \to |\downarrow\rangle$ are more likely to be dominated by spontaneous processes from coupling of the qubit to a thermal reservoir. On the other hand, for low temperatures, $k_B T \ll \hbar\omega_{ge}$, for $\omega_q - \omega_{ge}$ near the peaks of the correlator $\Phi_{\hat{n}\hat{n}}(\omega)$, the coupling-induced upward transitions $|\downarrow\rangle \to |\uparrow\rangle$ can have a considerable relative rate and determine the resulting population of the excited qubit state. Then the ratio of the heights of the peaks of $\Phi_{\hat{n}\hat{n}}(\omega)$ can be found from the ratio of the populations of the excited qubit state for the corresponding frequencies, which was measured in the experiment [30].

The experimental data [30] are compared with the theory in figure 2(a). The directly measured quantity was the population of the excited qubit state as a function of frequency ω_q. It displayed three peaks, the central one (at frequency $\approx \omega_{ge}$) and two sideband peaks on opposite sides. The ratio r_s of the populations of the small- and large-amplitude sideband peaks was then determined, and from it the effective Planck number $\bar{n}_e$ was extracted as $r_s/(1 - r_s)$.

The results of the experiment are in qualitative agreement with expression (14) for $\bar{n}_e$. The agreement improves for larger scaled field intensity β (4), where the ratio κ/ν_0 is smaller. It is in the range of small κ/ν_0 that the quantum temperature is a good characteristic of the

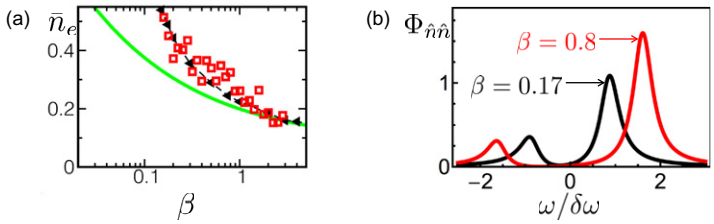

Figure 2. (a) Solid line: the Planck number $\bar{n}_e$ of the vibrations about the large-amplitude state of the modulated oscillator, which corresponds to the minimum of $g(Q, P)$ in the small-damping limit, equation (14) (see also [34]); β is the scaled driving field intensity (4), $\bar{n} = 0$. Squares: experimental data obtained from the ratio of the heights of the sideband spectral peaks [30], as explained in the text. Triangles: a theoretical estimate of the experimentally measured quantity obtained with no adjustable parameters. (b) The scaled power spectra of the oscillator occupation number $\hat{n} = a^\dagger a$ for vibrations about the large-amplitude stable state for $\kappa = 1/3.9$ (the value used in [30]). The black and red curves correspond to $\beta = 0.17$ and 0.8. The triangles in (a) are determined from the ratio r_Φ of the heights of the lower and higher peaks of $\Phi_{\hat{n}\hat{n}}$ as $r_\Phi/(1 - r_\Phi)$.

distribution over quasienergy states, as the lifetime of these states largely exceeds the reciprocal level spacing (scaled by $\hbar$). In this limit function $\Phi_{\hat{n}\hat{n}}(\omega)$ has distinct peaks that very weakly overlap, see figure 2(b).

To describe the experiment for larger κ/ν_0, one has to use the full theory that accounts for the overlap of the peaks of $\Phi_{\hat{n}\hat{n}}(\omega)$. We used the calculated $\Phi_{\hat{n}\hat{n}}(\omega)$ to find the ratio r_Φ of the peak heights. To match the experimental procedure, we found the effective $\bar{n}_e$ as $r_\Phi/(1 - r_\Phi)$. The result is shown in figure 2(a). It is in good agreement with the experiment, with no adjustable parameters.

4. Switching between the stable states

The effect of diffusion over quasienergy states due to quantum fluctuations is not limited to the narrow region close to the extrema of $g(Q, P)$. Along with small fluctuations that lead to a small change of quasienergy there occasionally occur large fluctuations. They push the oscillator far away from the initially occupied extremum of $g(Q, P)$. It is clear that, if as a result of such fluctuation, the oscillator goes 'over the quasienergy barrier' to states localized about the other extremum, with probability ≈ 1 it will then approach this other extremum. Such transition corresponds to switching between the stable states of forced vibrations. As mentioned before, since the switching occurs as a result of diffusion over quasienergy, we call the switching mechanism quantum activation. As seen from figure 1(a), with an accuracy to a factor $\sim 1/2$ the switching rate W_{sw} is determined by the probability of reaching the saddle-point value g_S of $g(Q.P)$.

The switching rate is small, as switching requires that the oscillator makes many interlevel transitions $m \to n$, $m < n$, with rates W_{mn} smaller than the rates of transitions in the opposite direction, W_{nm}. Therefore, before the oscillator switches, there is formed a quasistationary distribution over its states localized about the initially occupied extremum of $g(Q, P)$. This is similar to what happens in thermally activated switching over a high barrier [31]. However, in contrast to systems in thermal equilibrium, a modulated oscillator generally does not have detailed balance. Its statistical distribution has a simple Boltzmann form with temperature $\mathcal{T}_e$

only close to the extrema of $g(Q, P)$. Therefore the standard technique developed for finding the switching rate in quantum equilibrium systems [41–44] does not apply. Also, even for $T \to 0$ an oscillator modulated close to its eigenfrequency generally does not switch via tunneling (see [16, 19, 21, 45–49] for the theory of tunneling switching for additive and parametric modulation). Switching via quantum activation is exponentially more probable.

4.1. Relation to chemical kinetics and population dynamics

For small scaled decay rate κ the switching rate $W_{\rm sw}$ can be obtained from the balance equation (11). An approach to solving this equation was discussed earlier [15, 18]. Here we provide a formulation that gives an insight into how the oscillator actually moves in switching and also makes a direct connection with the technique developed in chemical kinetics and population dynamics. The balance equation is broadly used in these areas. It describes chemical or biochemical reactions in stirred reactors (no spatial nonuniformity). The reactions can be thought of as resulting from molecular collisions in which molecules transform, and if the collision duration is small compared to the reciprocal collision rate the kinetics is described by a Markov equation [50]

$$\dot{\rho}(\mathbf{X}, \tau) = \sum_{\mathbf{r}} [W(\mathbf{X} - \mathbf{r}, \mathbf{r})\rho(\mathbf{X} - \mathbf{r}, \tau) - W(\mathbf{X}, \mathbf{r})\rho(\mathbf{X}, \tau)]. \tag{16}$$

Here, $\mathbf{X} = (X_1, X_2, \ldots)$ is the vector that gives the numbers of molecules X_i of different types i and ρ is the probability for the system to be in a state with given $\mathbf{X}$; $W(\mathbf{X}, \mathbf{r})$ is the rate of a reaction in which the number of molecules changes from $\mathbf{X}$ to $\mathbf{X} + \mathbf{r}$. Typically, X_i are large, $X_i \propto N \gg 1$, where N is the total number of molecules. In contrast, the change of the number of molecules in an elementary collision is $|\mathbf{r}| \sim 1$, because it is unlikely that many molecules would collide at a time. Equation (16) is also often used in population dynamics, including epidemic models, cf [51]. In this case the components of $\mathbf{X}$ give populations of different species.

Since the number of molecules (population) is large, $N \gg 1$, fluctuations are small on average. Disregarding fluctuations corresponds to the mean-field approximation. In this approximation one can multiply (16) by $\mathbf{X}$ and sum over $\mathbf{X}$ while assuming that the width of the distribution $\rho(\mathbf{X})$ is small. This gives the equation of motion for the scaled mean number of molecules (population) $\bar{\mathbf{x}} = \overline{\mathbf{X}}/N$,

$$\dot{\bar{\mathbf{x}}} = \sum_{\mathbf{r}} \mathbf{r} w(\bar{\mathbf{x}}, \mathbf{r}), \quad \mathbf{x} = \mathbf{X}/N, \quad w(\mathbf{x}, \mathbf{r}) = W(\mathbf{X}, \mathbf{r})/N. \tag{17}$$

Stable solutions of (17) give the stable states of chemical (population) systems. There may be also unstable stationary or periodic states; an unstable stationary solution of (17) can be the state where one of the species goes extinct.

Equation (16) describes diffusion in the space of variables $\mathbf{x}$. Along with small ($\propto N^{-1/2}$) fluctuations around the stable states, this diffusion leads to rare large deviations ($\sim \mathcal{O}(1)$ in $\mathbf{x}$-space) and to switching between the stable states. There is an obvious similarity between diffusion over the number of molecules and diffusion over quasienergy states of a modulated oscillator, but there are also some subtle differences, which we discuss below. There is also an obvious difference, with profound consequences: in the case of an oscillator the transition rates W_{mn} (11), (12) are not limited to $|m - n| \sim 1$.

4.2. The eikonal approximation

The role of the large number of molecules (population) in a modulated oscillator is played by the reciprocal effective Planck constant λ^{-1}, which determines the number of states localized about the extrema of $g(Q, P)$, cf figure 1. For $\lambda \ll 1$ it is convenient to switch from the state number n to the classical mechanical action I for the Hamiltonian orbits $Q(\tau; g)$, $P(\tau; g)$, which are described by equations $\dot{Q} = \partial_P g(Q, P)$, $\dot{P} = -\partial_Q g(Q, P)$,

$$I = I(g) = (2\pi)^{-1} \int_0^{2\pi/\nu(g)} P(\tau; g)\dot{Q}(\tau; g)\, \mathrm{d}\tau, \quad \partial_g I = \nu^{-1}(g), \tag{18}$$

where $\nu(g)$ is the vibration frequency for given g ($2\pi I$ gives the area of the cross-section of the surface $g(Q, P)$ in figure 1(a) by plane $g = \text{const}$). One can show that, in spite of the nonstandard form of $g(Q, P)$, the semiclassical quantization condition has the familiar form $I_n \equiv I(g_n) = \lambda(n + 1/2)$.

In the semiclassical approximation the rates of transitions between quasienergy states W_{mn} become functions of the quasicontinuous variable I and can be written as $W_{mn} = W(I_m, n - m)$. The dependence of W on I is smooth, as seen from (11) and (12), $W(I_m, n - m) \approx W(I_n, n - m)$ for typical $|n - m| \ll 1/\lambda$.

Similar to (17), in the neglect of quantum fluctuations the equation for $\overline{I} = \sum_n I_n \rho_{nn}$ has a simple form

$$\dot{\overline{I}} = \sum_r r\, w(\overline{I}, r), \quad w(I, r) = \lambda W(I, r). \tag{19}$$

This equation shows how the oscillator is most likely to evolve. Using that the matrix element a_{mn} in the expression (11) for the rate W_{mn} is the $(m - n)$th Fourier component of function $(2\lambda)^{-1/2}[Q(\tau; g_m) + \mathrm{i}P(\tau; g_m)]$, one can show by invoking the Stokes' theorem that the time evolution of $\overline{I}$ is extremely simple,

$$\dot{\overline{I}} = -2\kappa \overline{I}, \quad \overline{I} < I_{\mathcal{S}}, \tag{20}$$

where $I_{\mathcal{S}}$ is the value of $I(g)$ for g approaching the saddle-point value $g_{\mathcal{S}}$ from the side of the considered extremum of $g(Q, P)$; the values of $I_{\mathcal{S}}$ are different on opposite sides of $g_{\mathcal{S}}$. Equation (20) coincides with the result for the evolution of $\overline{g} \equiv \overline{g}(\overline{I})$ for a classical modulated oscillator [3]. We note that the semiclassical approximation breaks down very close to the saddle point (in particular, the relation $W(I_m, n - m) \approx W(I_n, n - m)$ clearly ceases to apply), but the width of the corresponding range of I goes to zero as $\lambda \to 0$.

We now consider the distribution ρ_{nn} about the initially occupied stable state. This distribution is quasistationary on times small compared to the reciprocal switching rate. To find ρ_{nn} far from the stable state we use the eikonal approximation [15, 18], but in a form similar to that used in chemical kinetics and population dynamics [33]. Exploiting the correspondence $N \leftrightarrow 1/\lambda$, we set

$$\rho_{nn} = \exp[-R(I_n)/\lambda] \tag{21}$$

and assume that $|\partial_I R| \ll \lambda^{-1}$. Then $\rho_{n+r\,n+r} \approx \rho_{nn} \exp[-r\partial_I R]$ for $|r| \ll \lambda^{-1}$ and, to leading order in λ, the balance equation (11) becomes

$$\partial_\tau R = -\mathcal{H}(I, \partial_I R), \quad \mathcal{H}(I, p_I) = \sum_r w(I, r)[\exp(r p_I) - 1]. \tag{22}$$

Equation (22) justifies the ansatz (21). It has the form of the Hamilton–Jacobi equation for an auxiliary system with coordinate I, momentum p_I and action variable $R(I)$ [2]. It thus maps the problem of finding the distribution of the modulated oscillator, which is formed by quantum fluctuations, onto the problem of classical mechanics. The quasistationary distribution is determined by the stationary solution of (22), i.e. by the solution of equation $\mathcal{H}(I, \partial_I R) = 0$. If there are several solutions, of physical interest is the solution with the minimal $R(I)$, as it gives the leading-order term in $\ln \rho_{nn}$.

4.3. Optimal switching trajectory

An advantageous feature of the formulation (22) is that it provides an insight into how the quantum oscillator evolves in large fluctuations that form the tail of the distribution about the initially occupied extremum of $g(Q, P)$. Even though the diffusion over quasienergy states is a random process and different sequences of interstate transitions can bring the system to a given quasienergy state, the probabilities of such sequences are strongly different. Of physical interest is the most probable sequence, known as the optimal fluctuation. For classical fluctuating systems it has been understood theoretically and shown in experiment and simulations [33, 52–55] that the evolution of the system in the optimal fluctuation, i.e. the optimal fluctuation trajectory is given by the classical trajectory of the auxiliary Hamiltonian system with Hamiltonian $\mathcal{H}$. In the present context, this trajectory provides a minimum to $R(I)$ and thus the maximum to the probability distribution ρ_{nn} (21). It is described by equation

$$\dot{I} = \partial\mathcal{H}(I, p_I)/\partial p_I, \quad \dot{p}_I = -\partial\mathcal{H}(I, p_I)/\partial I; \quad R(I) = \int_0^I p_I \, \mathrm{d}I. \tag{23}$$

The concept of the classical optimal fluctuation trajectory extends to the quantum oscillator. Such a trajectory for the action variable I is well defined, since any information on the oscillator phase is erased in our formulation where off-diagonal matrix elements ρ_{mn} with $m \neq n$ are small and thus disregarded. The characteristic range of the I values, $0 \leqslant I \lesssim I_S$, largely exceeds the quantum uncertainty in I, which is $\propto \lambda$. Therefore the optimal fluctuation trajectory $I(t)$ can be measured in the experiment in the same way as is done in classical systems. The trajectory $I(t)$ corresponds to the optimal fluctuation trajectory of the quasienergy $g(t)$, since the I and g variables are related by $\partial_g I = \nu^{-1}(g)$.

In (23) we have set $R(0) = 0$ and thus ignored the normalization factor in the expression (21) for ρ_{nn}. This factor is ~ 1 and leads to a correction $\propto \lambda$ to $R(0)$. Since, to logarithmic accuracy, the switching rate is determined by the probability of approaching the saddle-point value I_S, we have

$$W_{\mathrm{sw}} \sim \kappa |\delta\omega| \exp(-R_{\mathrm{A}}/\lambda), \quad R_{\mathrm{A}} = R(I_S). \tag{24}$$

Parameter R_{A} plays the role of the effective activation energy for switching via quantum activation, with the effective Planck constant λ replacing the temperature in the conventional expression for thermally activated switching.

Large rare fluctuations start when the oscillator is near its stable state at the extremum of $g(Q, P)$, where $I = 0$. Therefore optimal trajectories start from $I = 0$, as reflected in (23). The value of the momentum $p_I \equiv \partial_I R$ for $I \to 0$ on the trajectory can be found by noticing that the distribution over quasienergy near the extremum of $g(Q, P)$ is of the form of the Boltzmann distribution with effective temperature $\mathcal{T}_{\mathrm{e}}$, and thus $R \propto I/\mathcal{T}_{\mathrm{e}}$; from (14) $p_I = \ln[(\bar{n}_{\mathrm{e}} + 1)/\bar{n}_{\mathrm{e}}]$ for $I \to 0$. Then from (22), $\dot{I} = 2\kappa I$ on the optimal fluctuation trajectory for $I \to 0$. As expected,

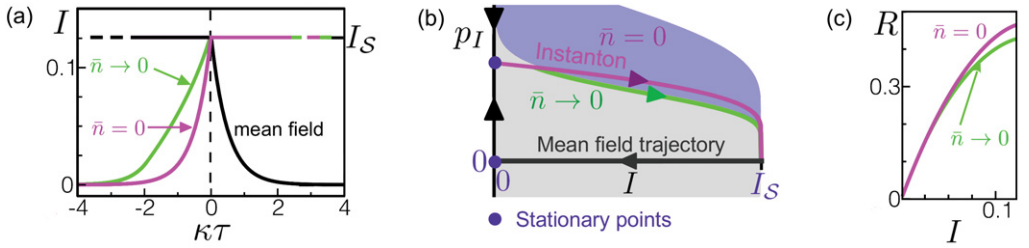

Figure 3. (a) The mean-field (fluctuation free) and optimal fluctuation trajectories of the action variable. Because for $\bar{n} = 0$ the system has detailed balance, the optimal trajectory in this case is the time-reversed mean-field trajectory. The data refer to the trajectories for the local maximum of $g(Q, P)$ in figure 1 for $\beta = 0.035$. The shape of the trajectory changes discontinuously where $\bar{n}$ becomes nonzero; the transition between the semiclassical limits $\bar{n} = 0$ and $\bar{n} \to 0$ occurs in the range $\exp(-c/\lambda) < \bar{n} \lesssim \lambda^{3/2}$, where the approximation leading to (22) breaks down [38] ($c = c(\beta) \sim 1$). (b) The phase portrait of the auxiliary Hamiltonian system that describes large fluctuations of the oscillator in the small-damping limit. The real-time instantons in (a) correspond to the trajectories in phase space of the same color. The gray area shows the region where $\mathcal{H}(I, p_I)$ remains finite for $\bar{n} \neq 0$; for $\bar{n} = 0$, $\mathcal{H}$ remains finite in the whole region shown in the figure. (c) The logarithm of the probability distribution $R(I_n) \approx -\lambda \ln \rho_{nn}$ for $\bar{n} = 0$ and $\bar{n} > 0$.

$\dot{I} > 0$, and thus the system moves along this trajectory away from the stable state of fluctuation-free dynamics.

The facts that $p_I \neq 0$ at the starting point of the optimal trajectory and that the state $I = 0$ lies on the boundary of the available values of I are connected with each other and present a distinctive feature of the oscillator dynamics. In chemical kinetics and population dynamics usually stable states lie in the middle of the space of dynamical variables $\mathbf{X}$. The probability distribution has a Gaussian maximum at such $\mathbf{X}$, and then the momentum on the optimal trajectory is equal to zero [28, 33]. In contrast, in the case of the oscillator the Hamiltonian $\mathcal{H}(I, p_I)$ has two stationary points with $I = 0$: $(I = 0, p_I = 0)$ and $(I = 0, p_I = \ln[(\bar{n}_e + 1)/\bar{n}_e])$. From (14), $\dot{I} = \dot{p}_I = 0$ at these points. The motion of the system near these points is exponential in time and is shown in figure 3. The state $(I = 0, p_I = 0)$ is asymptotically approached as $t \to \infty$ along the fluctuation-free trajectory (20), whereas $(I = 0, p_I = \ln[(\bar{n}_e + 1)/\bar{n}_e])$ is the starting point of the optimal fluctuation trajectory that goes away from $I = 0$.

Figure 3(a) shows the mean-field (fluctuation-free) trajectory $\bar{I}(t)$ and the optimal trajectory $I(t)$ obtained numerically from equations (20) and (23), respectively. An interesting feature of the considered model of the modulated quantum oscillator is that it satisfies the detailed balance condition for $\bar{n} = [\exp(\hbar\omega_0/k_B T) - 1]^{-1} = 0$ [27]. This is seen from the explicit expression for the rates (11) and (12), as for $\bar{n} = 0$ they meet the familiar detailed balance condition $W_{n\,n+k}/W_{n+k\,n} = \exp(-k/\xi_n)$ (the explicit form of $\xi_n \equiv \xi(I_n)$ follows from (12)). Therefore $p_I = 1/\xi(I)$, and one can show from (23) that $\dot{I} = 2\kappa I$ for all I. As a consequence, the optimal fluctuation trajectory $I(t)$ is the time-reversed mean-field trajectory $\bar{I}(t)$. This is a generic feature of classical systems with detailed balance, see [52]. Our results show that time-reversal symmetry also holds in quantum systems provided the notion of a trajectory is well defined.

Of special interest is the vicinity of the saddle-point value of the action variable I_S, see figure 3. In a dramatic distinction from reaction systems, there is no slowing down of $I(t)$ near I_S. The quantity I_S is a boundary value of I for states localized about a given extremum of $g(Q, P)$ in figure 1. Functions $\dot{\bar{I}}$ and $\dot{I}$ are discontinuous there. This is an artifact of the balance equation approximation, which assumes that the dimensionless frequency $\nu(g) \gg \kappa$. For $g \to g_S$ the frequency $\nu(g) \to 0$, and the approximation breaks down. With account taken of decay, in the region of bistability the oscillator has a 'true' unstable stationary state in the neglect of fluctuations. Both the mean-field trajectory and the optimal trajectory in phase space are moving away/approaching this state exponentially in time, cf [15], but the region of I where it happens is very narrow for small κ.

4.4. Fragility in the problem of large rare fluctuations

A striking feature of optimal fluctuation trajectories obvious from figure 3 is that these trajectories have different shapes depending on whether the oscillator Planck number is $\bar{n} = 0$ or $\bar{n} > 0$. The discontinuous with respect to $\bar{n}$ change of the trajectories and the associated change of the logarithm of the distribution $R(I)$ and of the activation energy for switching R_A show the fragility of the detailed-balance solution for $\bar{n} = 0$ [15, 18]. It has been found that the fragility also emerges in a very different type of problem, the problem of population dynamics described by equation (16) [28]. In particular, the well-known result for the rate of disease extinction in the presence of detailed balance [56–59] can change discontinuously with the varying elementary rates $W(\mathbf{X}, \mathbf{r})$ as the detailed balance is broken.

We now show that the condition for the onset of fragility proposed in [28] can be extended also to the modulated oscillator. The analysis [28] relied on the expression for the switching exponent in a reaction system. Similar to how it was done above for the oscillator, this exponent can be found by seeking the solution of the master equation (16) in the eikonal form $\rho(\mathbf{X}) = \exp[-N\tilde{R}(\mathbf{x})]$. To the leading order in $1/N$, the problem is then mapped onto Hamiltonian dynamics of an auxiliary system with mechanical action $\tilde{R}(\mathbf{x})$. From (16), the Hamiltonian of the auxiliary system is

$$\mathcal{H}(\mathbf{x}, \mathbf{p}) = \sum_{\mathbf{r}} w(\mathbf{x}, \mathbf{r})[\exp(\mathbf{rp}) - 1], \quad \mathbf{p} = \partial_{\mathbf{x}}\tilde{R} \tag{25}$$

(as before, we use that $W(\mathbf{X} - \mathbf{r}, \mathbf{r}) \approx W(\mathbf{X}, \mathbf{r}) \equiv N w(\mathbf{x}, \mathbf{r})$). If the system is initially near a stable state $\mathbf{x}_a$ (a stable solution of (17)), $\tilde{R}(\mathbf{x})$ is determined by the Hamiltonian trajectory that emanates from $\mathbf{x}_a$. From (25), $\tilde{R}(\mathbf{x}) = \int_{\mathbf{x}_a}^{\mathbf{x}} \mathbf{p}\, d\mathbf{x}$. The rate of switching from $\mathbf{x}_a$ (or extinction, in the extinction problem) is $W_{sw} \propto \exp(-N\tilde{R}_A)$,

$$\tilde{R}_A = \int_{\mathbf{x}_a}^{\mathbf{x}_S} \mathbf{p}\, d\mathbf{x} = \int dt\, \mathbf{p}(t)\dot{\mathbf{x}}(t)\, dt. \tag{26}$$

Here $\mathbf{x}_S$ is the saddle point of the deterministic dynamics (17); it can be shown that it is the Hamiltonian trajectory that goes to the saddle point that provides the switching or extinction exponent $\tilde{R}_A$, cf [3, 33, 60]. Both $\mathbf{x}_a$ and $\mathbf{x}_S$ are stationary points of the Hamiltonian $\mathcal{H}$, and the integral over time in (26) goes from $-\infty$ to ∞ ($\mathbf{x}_S$ is approached asymptotically as $t \to \infty$). This is a significant distinction from the modulated oscillator problem; there $\dot{I}$ is discontinuous

for $I \to I_S$ and equations (23) and (24) for the activation exponent can be written as

$$R_{\rm A} = \int_{-\infty}^{0} {\rm d}t\, p_I(t)\dot{I}(t),$$

where we set the instant where $I(t)$ reaches I_S on the optimal trajectory to be $t = 0$.

A small change of the reaction rates $W(\mathbf{X}, \mathbf{r}) \to W(\mathbf{X}, \mathbf{r}) + \epsilon W^{(1)}(\mathbf{X}, \mathbf{r})$ ($\epsilon \ll 1$) leads to the linear in ϵ change of the Hamiltonian, $\mathcal{H} \to \mathcal{H} + \epsilon\mathcal{H}^{(1)}$, as seen from (25). The action is then also changed. To the first order in ϵ, $\tilde{R}_{\rm A} \to \tilde{R}_{\rm A} + \epsilon\tilde{R}_{\rm A}^{(1)}$. The correction term is given by a simple expression familiar from the Hamiltonian mechanics [2],

$$\epsilon\tilde{R}_{\rm A}^{(1)} = -\epsilon\int {\rm d}t\mathcal{H}^{(1)}\Big(\mathbf{x}(t), \mathbf{p}(t)\Big), \quad \mathcal{H}^{(1)} = \sum_{\mathbf{r}} w^{(1)}(\mathbf{x}, \mathbf{r})(e^{\mathbf{pr}} - 1), \tag{27}$$

where the integral is calculated along the *unperturbed* trajectory $\mathbf{x}(t)$, $\mathbf{p}(t)$. In the extinction problem the integral (27) can diverge at the upper limit, $t \to \infty$. This is because in this problem $\mathbf{p}(t)$ remains finite for $t \to \infty$, and therefore if $w^{(1)}(\mathbf{x}_S, \mathbf{r})$ is nonzero, $\mathcal{H}^{(1)} \neq 0$ for $t \to \infty$. The divergence indicates the breakdown of the perturbation theory; in the particular example studied in [28], the difference between the values of $\tilde{R}_{\rm A}$ for $\epsilon = 0$ and $\epsilon \to 0$ was $\sim \tilde{R}_{\rm A}$.

For the modulated oscillator, the role of the small parameter ϵ is played by the Planck number $\bar{n}$. If $w^{(0)}(I, r)$ is the transition rate for $\bar{n} = 0$, then from (11) the thermally induced term in the transition rate has the form $\bar{n}w^{(1)}(I, r) = \bar{n}[w^{(0)}(I, r) + w^{(0)}(I, -r)]$. Where the perturbation theory applies, the correction to the effective activation energy of switching reads

$$\bar{n}R_{\rm A}^{(1)} = -\bar{n}\int_{-\infty}^{0} {\rm d}t \sum_{r} w^{(1)}\Big(I(t), r\Big)\{\exp[rp_I(t)] - 1\}. \tag{28}$$

As we saw, in contrast to reaction systems, $p_I \neq 0$ for $t \to -\infty$. However, $w^{(1)}(I, r) \propto I \propto \exp(2\kappa t)$ for $t \to -\infty$, therefore (28) does not diverge for $t \to -\infty$. There is also no accumulation of perturbation for large t, as the integral goes to $t = 0$. Therefore the cause of the fragility should be different from that in reaction systems.

As mentioned earlier, in contrast to reaction systems, for the oscillator the values of r in (28) can be large. Then the correction $R_{\rm A}^{(1)}$ can diverge because of the divergence of the sum over r. This happens if on the optimal trajectory $w^{(1)}(I, r)$ decays with r slower than $\exp(-rp_I)$. From (12), $w^{(1)}(I, r)$ decays with r exponentially; in particular, $w^{(1)}(I, r) \propto \exp[-2r\nu(g)\tau_*(g)]$ for $r \gg 1$ (here, g is related to I by equation (18)). The region of the values of p_I where $\sum_r w^{(1)}(I, r)\exp(rp_I)$ remains finite is shown in figure 3(b). As seen from this figure, even though $p_I \sim 1$, its value on the $\bar{n} = 0$-trajectory can be too large for the sum over r to converge. Then the perturbation theory becomes inapplicable. The trajectory followed in switching changes discontinuously where $\bar{n}$ changes from $\bar{n} = 0$ to $\bar{n} > 0$. The probability distribution also changes discontinuously.

An important problem is the crossover between the instanton solutions without and in the presence of the perturbation. For a modulated quantum oscillator it was recently addressed in [38] (but the most probable fluctuational trajectories were not studied in this paper). The analysis [38] shows that the very instanton approximation breaks down by thermal fluctuations, function $\partial_I R$ is not smooth, rather it displays a kink. The threshold for the onset of this behavior is exponentially low in $\bar{n}$, with $|\ln\bar{n}| \lesssim \lambda^{-1}$. It corresponds to the regime where the rate of transitions between oscillator states induced by absorption of thermal excitations, which is $\propto \bar{n}$,

becomes comparable with the switching rate $W_{\rm sw}$ calculated for $\bar{n} = 0$. The region where the instanton approximation is inapplicable extends to $\bar{n} \lesssim \lambda^{3/2}$.

To conclude this section, we note that the instanton approximation relies on the assumption that the mean square fluctuations provide the smallest scale in the problem, similar to the wavelength in the WKB approximation [39]. If the system is perturbed and the perturbation is small, it can be incorporated into the prefactor of the rate of rare large fluctuations. If the perturbation is still small but exceeds the small parameter of the theory, it can be incorporated into the instanton Hamiltonian and leads to a correction to the exponent of the rare event rates. This correction is generically linear in the perturbation. However, this is apparently not universal behavior, as the unperturbed solution can be fragile with respect to a perturbation. So far the fragility has been found in cases where the perturbation breaks the time-reversal symmetry.

5. Nonresonant modulation: microscopic mechanisms of heating and cooling

Much attention has been attracted recently by the possibility of manipulating the probability distribution of mesoscopic oscillators by external drive, and a whole new area, cavity optomechanics, has emerged, see [61] for a recent review. The primary goal is to cool the oscillators, but heating is also possible, as well as pumping into the state of self-sustained vibrations. In contrast to the quantum heating discussed above, here oscillators are modulated nonresonantly. The modulation frequency $\omega_{\rm F}$ significantly differs from the oscillator frequency ω_0. Still, the effect comes from the interplay of modulation and quantum fluctuations in the thermal reservoir, and in this section we briefly discuss various mechanisms that lead to this effect. As we show, these mechanisms can be described in unifying terms. It will be seen that they are similar to the mechanism discussed in section 3.3 in the analysis of the experimental observation of the quantum heating, as we remarked there.

The very idea of cooling quantum systems with discrete energy spectrum by a high-frequency field goes back to the mid-1970s [62–64], about the same time that the laser cooling of atomic motion was proposed [65, 66]. The change of the distribution can be understood from figure 4 [37, 62–64]. It refers to a system coupled by the modulating field to another system, which can be a thermal bath or a mode with a relaxation time much shorter than that of the system of interest, so that it serves effectively as a narrow-band thermal reservoir. The modulation provides a new channel of relaxation for the relatively slowly relaxing system of interest.

Figure 4 indicates possible transitions between the states of the system accompanied by energy exchange with the thermal reservoir. For example in (a), a transition of the system from the excited to the ground state is accompanied by a transition of the reservoir to the excited state with energy $\hbar\omega_{\rm b} = \hbar(\omega_0 + \omega_{\rm F})$, with the energy deficit compensated by the modulation. On the other hand, a transition of the system from the ground to the excited state requires absorbing an excitation in the thermal reservoir, which is possible only when such excitation is present in the first place. The ratio of the state populations of the system is determined by the ratio of the rates of transitions up and down in energy, and thus by the population of the excited states of the thermal reservoir with energy $\hbar\omega_{\rm b}$. In the analysis of section 3.3 the system was a qubit whereas the role of the energy levels of the reservoir was played by the oscillator quasienergy levels.

If the corresponding process is the leading relaxation process, the effective temperature of the system becomes $T^* = (\omega_0/\omega_{\rm b})T$. It means there occurs effective cooling for $\omega_0 \ll \omega_{\rm b}$. Similarly, for $\omega_0 \gg \omega_{\rm b}$ the modulation leads to heating of the system, see figure 4(b). In the

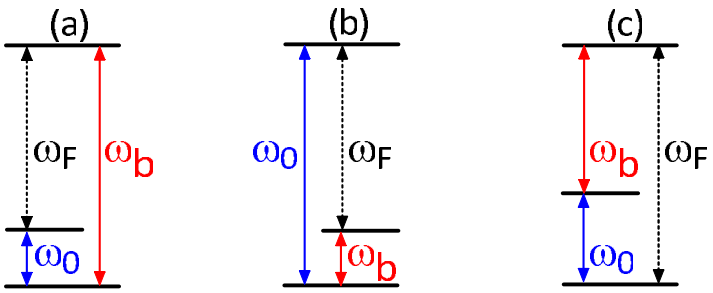

Figure 4. Modulation-induced relaxation processes leading to cooling (a), heating (b) and population inversion (c); ω_0, ω_F and ω_b are the frequency of the system (the oscillator, in the present case), the modulation frequency and the frequency of the mode (or a thermal bath excitation) to which the oscillator is coupled by the modulation, respectively; the relaxation time of the mode is much shorter than that of the oscillator. Strong modulation imposes on the oscillator the probability distribution of the fast-decaying mode in (a) and (b) and leads to population inversion in (c). If, in the absence of modulation, oscillator relaxation is described by the standard linear friction model (6), (7), the distribution over the Fock states in the presence of modulation is of the form of the Boltzmann distribution [64]; in (c) the distribution over low-energy Fock states is described by negative temperature and the oscillator performs self-sustained vibrations close to its eigenfrequency.

case sketched in figure 4(c), the induced transitions from the ground to the excited state of the system are more probable then from the excited to the ground state, which leads to a negative effective temperature for strong modulation.

In the case of an oscillator, the system has many levels, but the above picture still applies. The unexpected feature is that the distribution of the oscillator over its Fock states can be of the Boltzmann form with an effective temperature determined by the strength and frequency of the modulation [64], see below.

A simple model of the modulation-induced dissipation is where the external field parametrically modulates the coupling of the oscillator to a thermal bath. The coupling Hamiltonian is

$$H_i^{(\mathrm{F})} = -qh_{\mathrm{b}}^{(\mathrm{F})} A\cos\omega_{\mathrm{F}} t. \tag{29}$$

Here, $h_{\mathrm{b}}^{(\mathrm{F})}$ depends on the variables of a thermal bath, or it can be the coordinate of a comparatively quickly decaying mode coupled to a thermal bath. Hamiltonian (29) is analogous to the field-induced term in the Hamiltonian of the qubit coupled to the oscillator (15), with the role of the oscillator coordinate played by the qubit operators $\sigma_\pm$ and the role of h_{b} played by $\hat{n}$.

The interaction (29) has the same structure as the interaction (6), except that it can lead to decay processes with the energy transfer $\hbar(\omega_0 \pm \omega_{\mathrm{F}})$, cf figures 4(a) and (b). Therefore the structure of the master equation for the oscillator should not change, but the decay parameters and the Planck numbers of excitations created in decay should change appropriately. The interaction can also lead to decay processes with energy transfer $\omega_{\mathrm{F}} - \omega_0$, for the appropriate modulation frequencies. In this case absorption of bath excitations is accompanied by oscillator transitions down in energy. Respectively, in the master equation (7) in the expression for the rates of transitions due to excitation absorption one has to formally replace $\bar{n}(\omega_0) \to \bar{n}(\omega_0 - \omega_{\mathrm{F}}) = -\bar{n}(\omega_{\mathrm{F}} - \omega_0) - 1$, which means that the friction coefficient becomes negative.

The above qualitative arguments can be confirmed by a formal analysis similar to that in [64]. It shows that in the RWA, the dissipation term in the master equation for the oscillator with account taken of the modulation-induced relaxation processes has the form (7) with the relaxation parameter Γ and the Planck number $\bar{n}$ replaced by $\Gamma_{\rm F} = \Gamma + \Gamma_+ + \Gamma_- - \Gamma_{\rm inv}$ and $\bar{n}_{\rm F}$,

$$(\partial_t \rho)_{\rm diss} = -\Gamma_{\rm F}(\bar{n}_{\rm F}+1)(a^\dagger a\rho - 2a\rho a^\dagger + \rho a^\dagger a) - \Gamma_{\rm F}\bar{n}_{\rm F}(aa^\dagger\rho - 2a^\dagger\rho a + \rho aa^\dagger), \tag{30}$$

where

$$\Gamma_{\pm,{\rm inv}} = \frac{A^2}{8\hbar\omega_0}\left|{\rm Re}\int_0^\infty {\rm d}t\,\langle[h_{\rm b}^{(2)}(t), h_{\rm b}^{(2)}(0)]\rangle_{\rm b}\,{\rm e}^{{\rm i}(\omega_0\pm\omega_{\rm F})t}\right|,$$
$$\bar{n}_{\rm F} = \{\Gamma\bar{n}(\omega_0) + \Gamma_+\bar{n}(\omega_0+\omega_{\rm F}) + \Gamma_-\bar{n}(\omega_0-\omega_{\rm F}) + \Gamma_{\rm inv}\,[\bar{n}(\omega_{\rm F}-\omega_0)+1]\}\,/\,\Gamma_{\rm F}. \tag{31}$$

Here, $\Gamma_\pm$ give the rates of transitions at frequencies $\omega_0 \pm \omega_{\rm F}$ sketched in figures 4(a) and (b); $\Gamma_{\rm inv}$ gives the rate of processes sketched in figure 4(c). If these latter processes dominate, they lead to vibrations of the oscillator at frequency $\approx\omega_0$, with amplitude determined by other mechanisms of losses [37]. Parameters Γ_- and $\Gamma_{\rm inv}$ in (31) refer to the cases where $\omega_0 > \omega_{\rm F}$ (red-shifted modulation) and $\omega_0 < \omega_{\rm F}$ (blue-shifted modulation), respectively; only one of these terms should be taken into account in (31). From (30) and (31), the probability distribution of the oscillator is characterized by effective temperature $T_{\rm F} = \hbar\omega_0/k_{\rm B}\ln[(\bar{n}_{\rm F}+1)/\bar{n}_{\rm F}]$.

Similar behavior occurs if the modulation is performed by an additive force $A\cos\omega_{\rm F}t$, but the interaction with the thermal reservoir is nonlinear in the oscillator coordinate, $H_i^{(2)} = q^2 h_{\rm b}^{(2)}$. This case was considered in [64]. It reduces to the above formulation if one makes a canonical transformation $U(t) = \exp[v^*(t)a - v(t)a^\dagger]$ (here time ordering is implied) with $v(t) = A_{\rm osc}(2\hbar\omega_0)^{-1/2}(-\omega_0\cos\omega_{\rm F}t + {\rm i}\omega_{\rm F}\sin\omega_{\rm F}t)$, where $A_{\rm osc} = A/(\omega_0^2 - \omega_{\rm F}^2)$ is the amplitude of forced vibrations of the oscillator. Indeed, as a result of this transformation $H_i^{(2)}$ transforms into $H_i^{({\rm F})}$ in which the field amplitude A is replaced with $-2A_{\rm osc}$ and $h_{\rm b}^{({\rm F})}$ is replaced with $h_{\rm b}^{(2)}$.

The analysis of cooling of a vibrating mirror in an optical cavity can also often be mapped onto the analysis of the interaction model (29). A quantum theory in this case was developed in [67, 68]. It considers an oscillator (the mirror) coupled to a cavity mode driven by external radiation. If the radiation is classical, in the appropriately scaled variables the coupling and modulation are described by Hamiltonians $H_i^{({\rm m})}$ and $H_{\rm F}^{({\rm m})}$, respectively,

$$H_i^{({\rm m})} = c_{\rm b} q q_{\rm b}^2, \quad H_{\rm F}^{({\rm m})} = -q_{\rm b} A\cos\omega_{\rm F}t, \tag{32}$$

where q and $q_{\rm b}$ are the coordinates of the mirror and the mode. In cavity optomechanics one usually writes $H_i^{({\rm m})} = c_{\rm b} q a_{\rm b}^\dagger a_{\rm b}$, because the mode frequency is much higher than ω_0 and the contributions from the terms $\propto a_{\rm b}^2$, $(a_{\rm b}^\dagger)^2$ is small; the discussion below trivially extends to this case.

In the absence of coupling to the mirror, the cavity mode is a linear system, hence $q_{\rm b}(t) = q_{{\rm b}0}(t) + [\chi_{\rm b}(\omega_{\rm F})\exp(-{\rm i}\omega_{\rm F}t) + {\rm c.c.}]A/2$, where $q_{{\rm b}0}(t)$ is the mode coordinate in the absence of modulation and $\chi_{\rm b}(\omega)$ is the susceptibility of the mode [68]. The coupling $H_i^{({\rm m})}$ in the interaction representation then has a cross-term $\propto Aq(t)q_{{\rm b}0}(t)\exp(\pm{\rm i}\omega_{\rm F}t)$. If the decay rate of the cavity mode is higher than that of the mirror, the mode then serves as a thermal bath for the mirror and the aforementioned cross-term is fully analogous to $H_i^{({\rm F})}$, with $q_{{\rm b}0}$ playing the role of $h_{\rm b}^{({\rm F})}$. Depending on the mode power spectrum at frequencies $\omega_{\rm F} \pm \omega_0$, modulation (32) can lead to cooling or pumping of the mirror vibrations, cf (31).

To conclude this section, here we have discussed three mechanisms that lead to the change of the oscillator distribution by nonresonant modulation: the dependence of the coupling to the field that drives the oscillator on the variables of the reservoir (or a mode with a short relaxation time), the nonlinearity of the coupling to the reservoir in the oscillator coordinate and the nonlinearity of the coupling to a fast-relaxing modulated mode in the dynamical variables of this mode. All these mechanisms are described in a unified way. Remarkably, for all of them the distribution of the oscillator over its Fock states is characterized by an effective temperature if the oscillator decay in the absence of the modulation corresponds to linear friction.

6. Conclusions

It follows from the results of this paper that a modulated nonlinear oscillator displays a number of quantum fluctuation phenomena that have no analogue in systems in thermal equilibrium. Oscillator relaxation is accompanied by a nonequilibrium quantum noise. It leads to a finite-width distribution of the oscillator over its quasienergy states even for the bath temperature $T \to 0$. For resonant modulation, the distribution is Boltzmann-like near the maximum. We have discussed the recent experiment that confirmed this prediction and the effect of oscillator damping on the outcome of a sideband-spectroscopy based measurement of the distribution.

The quantum noise also leads to large rare events that determine the far tail of the distribution of the resonantly modulated oscillator over quasienergy and to switching between the coexisting states of forced vibrations. We have developed an approach to the analysis of the distribution tail and the switching rate, which makes a direct connection with the analysis of the corresponding problems in chemical and biological systems and in population dynamics. We show that, in a large deviation, the quasienergy of an underdamped oscillator most likely follows a well-defined *real* trajectory in *real* time. This quantum trajectory is accessible to measurement. For $T = 0$, where the oscillator has detailed balance, the most probable fluctuation trajectory is the time-reversed trajectory of the fluctuation-free (mean-field) relaxation of the oscillator to the stable state. Thermal fluctuations break the detailed balance condition and, even where the thermal Planck number $\bar{n}$ is small compared to the effective Planck constant, lead to an $\bar{n}$-independent change of the most probable fluctuation trajectory.

A discontinuous change of the most probable trajectory with the varying parameter is the effect of fragility in the physics of rare events. We show that the criterion of the onset of fragility can be formulated in a general form that applies both to reaction systems with classical fluctuations and to the modulated quantum oscillator.

A nonresonant modulation can also change the probability distribution of the oscillator. Here the major mechanism is the effect of the modulation on the elementary quantum processes leading to oscillator decay and excitation. We have considered three major mechanisms of the effect and demonstrated that they can be described in a unified way. Depending on the modulation frequency and the power spectrum of the effective thermal reservoir responsible for the relaxation, nonresonant modulation can lead to heating, cooling or excitation of self-sustained vibrations of the oscillator. Interestingly, the distribution over the Fock states of a modulated oscillator is of the Boltzmann form with the effective temperature determined by the modulation, in a broad range of oscillator energies.

Acknowledgments

We are grateful to P Bertet and V N Smelyanskiy for the discussion. This research was supported in part by the ARO, grant W911NF-12-1-0235, and the Dynamics Enabled Frequency Sources program of DARPA. VP also acknowledges support from the ERC Starting grant OPTOMECH.

Appendix. Power spectrum of the occupation number of a modulated oscillator

For a periodically modulated oscillator, the fluctuation spectrum of operators K and L can be defined as

$$\langle\langle K, L\rangle\rangle_\omega = \int_0^\infty \mathrm{d}t\, \mathrm{e}^{\mathrm{i}\omega t}\langle\langle K(t)L(0)\rangle\rangle,$$

$$\langle\langle K(t)L(0)\rangle\rangle = \frac{\omega_\mathrm{F}}{2\pi}\int_0^{2\pi/\omega_\mathrm{F}} \mathrm{d}t_i\langle[K(t+t_i)-\langle K(t+t_i)\rangle][L(t_i)-\langle L(t_i)\rangle]\rangle. \tag{A.1}$$

The major contribution to this spectrum comes from small-amplitude fluctuations about the stable states of forced vibrations. We will not consider fluctuation-induced transitions between the stable states and will calculate the correlator (A.1) for each of these states separately; the averaging $\langle\ldots\rangle$ then means averaging over small-amplitude fluctuations about the corresponding state. We will not confine ourselves to the small-damping limit; moreover, we will assume that the scaled damping rate $\kappa \gg \lambda$, so that the spectra do not display the fine structure related to the nonequidistance of the levels g_n near the stable states [29, 34].

Of immediate interest to us is the spectrum of the operator $\hat{n} = a^\dagger a$ and in particular its scaled power spectrum $\Phi_{\hat{n}\hat{n}}(\omega)$,

$$\Phi_{\hat{n}\hat{n}}(\omega) = \lambda\,|\delta\omega|\,\mathrm{Re}\,\langle\langle\hat{n},\hat{n}\rangle\rangle_\omega; \quad \hat{n} = a^\dagger a \equiv (2\lambda)^{-1}(Q^2+P^2) - \tfrac{1}{2}. \tag{A.2}$$

Operator $\hat{n}$ does not have fast-oscillating factors $\propto \exp(\pm\mathrm{i}\omega_0 t)$. However, as seen from equation (13), for small decay rate $\hat{n}(t)$ contains terms which oscillate at frequencies $\sim \nu_0\delta\omega$ and $\sim 2\nu_0\delta\omega$ with ν_0 being the dimensionless frequency of vibrations about the considered stable state.

To find the correlator $\langle\langle\hat{n},\hat{n}\rangle\rangle_\omega$, we expand operators Q and P in (A.2) about the values of Q and P at the stable state, $Q = Q_\mathrm{a} + \delta Q$, $P = P_\mathrm{a} + \delta P$. To the leading order in $\lambda \ll 1$ we keep in $\hat{n}$ the terms linear in δQ, δP, which gives

$$\lambda^2\langle\langle\hat{n},\hat{n}\rangle\rangle_\omega \approx Q_\mathrm{a}^2\langle\langle\delta Q,\delta Q\rangle\rangle_\omega + Q_\mathrm{a}P_\mathrm{a}\Big(\langle\langle\delta Q,\delta P\rangle\rangle_\omega + \langle\langle\delta P,\delta Q\rangle\rangle_\omega\Big) + P_\mathrm{a}^2\langle\langle\delta P,\delta P\rangle\rangle_\omega. \tag{A.3}$$

In the same small-λ approximation, the correlators in equation (A.3) can be calculated from the master equation (7) in the Wigner representation; this method was used earlier [69] to find two linear combinations of them. Alternatively, and in a simpler way, they can be found from linearized equations of motion (9) complemented by quantum noise [34, 36],

$$\begin{aligned}&\delta\dot{Q} = K_{QQ}\delta Q + K_{QP}\delta P + \hat{f}_Q(\tau), \quad \delta\dot{P} = K_{PQ}\delta Q + K_{PP}\delta P + \hat{f}_P(\tau),\\ &\langle\hat{f}_Q(\tau)\hat{f}_Q(\tau')\rangle = \langle\hat{f}_P(\tau)\hat{f}_P(\tau')\rangle = \lambda\kappa(2\bar{n}+1)\delta(\tau-\tau').\end{aligned} \tag{A.4}$$

Here, $K_{QQ} = -\kappa + \partial_P\partial_Q g$, $K_{QP} = \partial_P^2 g$, $K_{PQ} = -\partial_Q^2 g$, $K_{PP} = -\kappa - \partial_Q\partial_P g$, where all derivatives are calculated at the stable state $(Q_\mathrm{a}, P_\mathrm{a})$. The commutation relation between the

random force components is $\langle[\hat{f}_Q(\tau), \hat{f}_P(\tau')]\rangle = 2i\lambda\kappa\delta(\tau-\tau')$. The noise correlator can be understood by noticing that the noise comes from the coupling to the bath and is not affected by the modulation or the oscillator nonlinearity [34]. Therefore it is the same as for a linear oscillator with no modulation, i.e. for $g=0$. In particular, the noise components $\hat{f}_Q$ and $\hat{f}_P$ anti-commute.

Multiplying equations (A.4) for $\delta\dot{Q}(\tau)$, $\delta\dot{P}(\tau)$ by $\exp[i(\omega/|\delta\omega|)\tau]$ and in turn by $\delta Q(0)$ and $\delta P(0)$, integrating then over τ by parts, and averaging, we will obtain a system of four linear algebraic equations for the correlators of δQ and δP in expression (A.3). The nonuniform part of these equations is given by the averages $\langle\delta Q^2\rangle$, $\langle\delta P^2\rangle$ and $\langle\delta Q\delta P+\delta P\delta Q\rangle$. They can be found from a system of linear equations that are obtained from (A.4) using the Stratonovich convention while keeping track of the order of the operators; for example, $\langle\delta Q(\tau)\hat{f}_Q(\tau)+\hat{f}_Q(\tau)\delta Q(\tau)\rangle = \lambda\kappa(2\bar{n}+1)$.

The resulting system of seven linear algebraic equations is trivially solved numerically. We used the solution to obtain $\Phi_{\hat{n}\hat{n}}(\omega)$ plotted in figure 2(b) and to calculate the ratio of the heights of the peaks of $\Phi_{\hat{n}\hat{n}}(\omega)$ used in figure 2(a).

We note that our minimalist model of the qubit–oscillator coupling leads also to the occurrence of a small peak in the population of the excited state of the qubit for $|\omega_q-\omega_{ge}|$ close to $2\nu_a|\delta\omega|$, which was reported in [30]. This peak can be related to the peak in the power spectrum of $\langle\langle\hat{n},\hat{n}\rangle\rangle_\omega$ for $\omega\sim 2\nu_0|\delta\omega|$, which results from the terms in $\hat{n}$ that are quadratic in δQ, δP; a contribution to this peak comes also from the anharmonicity of the oscillator vibrations about the stable state, i.e. from the higher-order terms in the expansion of $g(Q,P)$ in $Q-Q_a$, $P-P_a$ [70].

References

[1] Dykman M I (ed) 2012 *Fluctuating Nonlinear Oscillators: From Nanomechanics to Quantum Superconducting Circuits* (Oxford: Oxford University Press)
[2] Landau L D and Lifshitz E M 2004 *Mechanics* 3rd edn (Amsterdam: Elsevier)
[3] Dykman M I and Krivoglaz M A 1979 *Zh. Eksp. Teor. Fiz.* **77** 60–73
[4] Dmitriev A P and Dyakonov M I 1986 *Zh. Eksp. Teor. Fiz.* **90** 1430–40
[5] Kautz R L 1988 *Phys. Rev.* A **38** 2066–80
[6] Vogel K and Risken H 1990 *Phys. Rev.* A **42** 627–38
[7] Dykman M I, Maloney C M, Smelyanskiy V N and Silverstein M 1998 *Phys. Rev.* E **57** 5202–12
[8] Lapidus L J, Enzer D and Gabrielse G 1999 *Phys. Rev. Lett.* **83** 899–902
[9] Siddiqi I *et al* 2005 *Phys. Rev. Lett.* **94** 027005
[10] Kim K, Heo M S, Lee K H, Ha H J, Jang K, Noh H R and Jhe W 2005 *Phys. Rev.* A **72** 053402
[11] Aldridge J S and Cleland A N 2005 *Phys. Rev. Lett.* **94** 156403
[12] Stambaugh C and Chan H B 2006 *Phys. Rev.* B **73** 172302
[13] Almog R, Zaitsev S, Shtempluck O and Buks E 2007 *Appl. Phys. Lett.* **90** 013508
[14] Mahboob I, Froitier C and Yamaguchi H 2010 *Appl. Phys. Lett.* **96** 213103
[15] Dykman M I and Smelyanskii V N 1988 *Zh. Eksp. Teor. Fiz.* **94** 61–74
[16] Vogel K and Risken H 1988 *Phys. Rev.* A **38** 2409–22
[17] Kinsler P and Drummond P D 1991 *Phys. Rev.* A **43** 6194–208
[18] Marthaler M and Dykman M I 2006 *Phys. Rev.* A **73** 042108
[19] Peano V and Thorwart M 2006 *Chem. Phys.* **322** 135–43
[20] Katz I, Retzker A, Straub R and Lifshitz R 2007 *Phys. Rev. Lett.* **99** 040404
[21] Serban I and Wilhelm F K 2007 *Phys. Rev. Lett.* **99** 137001

[22] Vijay R, Devoret M H and Siddiqi I 2009 *Rev. Sci. Instrum.* **80** 111101
[23] Mallet F, Ong F R, Palacios-Laloy A, Nguyen F, Bertet P, Vion D and Esteve D 2009 *Nature Phys.* **5** 791–5
[24] Peano V and Thorwart M 2010 *Europhys. Lett.* **89** 17008
[25] Wilson C M, Duty T, Sandberg M, Persson F, Shumeiko V and Delsing P 2010 *Phys. Rev. Lett.* **105** 233907
[26] Verso A and Ankerhold J 2010 *Phys. Rev.* E **82** 051116
[27] Drummond P D and Walls D F 1980 *J. Phys. A: Math. Gen.* **13** 725–41
[28] Khasin M and Dykman M I 2009 *Phys. Rev. Lett.* **103** 068101
[29] Dykman M I, Marthaler M and Peano V 2011 *Phys. Rev.* A **83** 052115
[30] Ong F R, Boissonneault M, Mallet F, Doherty A C, Blais A, Vion D, Esteve D and Bertet P 2013 *Phys. Rev. Lett.* **110** 047001
[31] Kramers H 1940 *Physica (Utrecht)* **7** 284–304
[32] Touchette H 2009 *Phys. Rep.* **478** 1–69
[33] Kamenev A 2011 *Field Theory of Non-Equilibrium Systems* (Cambridge: Cambridge University Press)
[34] Dykman M I 2012 *Fluctuating Nonlinear Oscillators: From Nanomechanics to Quantum Superconducting Circuits* ed M I Dykman (Oxford: Oxford University Press) pp 165–97
[35] Schwinger J 1961 *J. Math. Phys.* **2** 407
[36] Mandel L and Camridge W E 1995 *Optical Coherence and Quantum Optics* (Cambridge: Cambridge University Press)
[37] Dykman M I and Krivoglaz M A 1984 *Soviet Physics Reviews* vol 5, ed I M Khalatnikov (New York: Harwood Academic) pp 265–441
[38] Guo L, Peano V, Marthaler M and Dykman M I 2013 *Phys. Rev.* A **87** 062117
[39] Landau L D and Lifshitz E M 1997 *Quantum Mechanics. Non-Relativistic Theory* 3rd edn (Oxford: Butterworth-Heinemann)
[40] Bertet P, Ong F R, Boissonneault M, Bolduc A, Mallet F, Doherty A C, Blais A, Vion D and Esteve D 2012 *Fluctuating Nonlinear Oscillators: From Nanomechanics to Quantum Superconducting Circuits* ed M I Dykman (Oxford: Oxford University Press) pp 1–31
[41] Langer J S 1967 *Ann. Phys.* **41** 108–57
[42] Coleman S 1977 *Phys. Rev.* D **15** 2929–36
[43] Affleck I 1981 *Phys. Rev. Lett.* **46** 388–91
[44] Caldeira A O and Leggett A J 1983 *Ann. Phys.* **149** 374–456
[45] Larsen D M and Bloembergen N 1976 *Opt. Commun.* **17** 254–8
[46] Sazonov V N and Finkelstein V I 1976 *Dokl. Akad. Nauk SSSR* **231** 78–81
[47] Dmitriev A P and Dyakonov M I 1986 *JETP Lett.* **44** 84–7
[48] Wielinga B and Milburn G J 1993 *Phys. Rev.* A **48** 2494–6
[49] Marthaler M and Dykman M I 2007 *Phys. Rev.* A **76** 010102R
[50] Van Kampen N G 2007 *Stochastic Processes in Physics and Chemistry* 3rd edn (Amsterdam: Elsevier)
[51] Anderson R M and May R M 1991 *Infectious Diseases of Humans: Dynamics and Control* (Oxford: Oxford University Press)
[52] Luchinsky D G and McClintock P V E 1997 *Nature* **389** 463–6
[53] Hales J, Zhukov A, Roy R and Dykman M I 2000 *Phys. Rev. Lett.* **85** 78–81
[54] Ray W, Lam W S, Guzdar P N and Roy R 2006 *Phys. Rev.* E **73** 026219
[55] Chan H B, Dykman M I and Stambaugh C 2008 *Phys. Rev. Lett.* **100** 130602
[56] Weiss G H and Dishon M 1971 *Math. Biosci.* **11** 261–5
[57] Leigh E G J 1981 *J. Theor. Biol.* **90** 213–39
[58] Jacquez J A and Simon C P 1993 *Math. Biosci.* **117** 77–125
[59] Doering C R, Sargsyan K V and Smereka P 2005 *Phys. Lett.* A **344** 149–55
[60] van Herwaarden O A and Grasman J 1995 *J. Math. Biol.* **33** 581–601
[61] Aspelmeyer M, Kippenberg T J and Marquardt F 2013 arXiv:1303.0733
[62] Zeldovich Y B 1974 *JETP Lett.* **19** 74–5

[63] Shapiro V E 1976 *Zh. Eksp. Teor. Fiz.* **70** 1463–76
[64] Dykman M I 1978 *Sov. Phys.—Solid State* **20** 1306–11
[65] Hänsch T W and Schawlow A L 1975 *Opt. Commun.* **13** 68
[66] Wineland D and Dehmelt H 1975 *Bull. Am. Phys. Soc.* **20** 637
[67] Wilson-Rae I, Nooshi N, Zwerger W and Kippenberg T J 2007 *Phys. Rev. Lett.* **99** 093901
[68] Marquardt F, Chen J P, Clerk A A and Girvin S M 2007 *Phys. Rev. Lett.* **99** 093902
[69] Serban I, Dykman M I and Wilhelm F K 2010 *Phys. Rev.* A **81** 022305
[70] André S, Guo L, Peano V, Marthaler M and Schön G 2012 *Phys. Rev.* A **85** 053825